Acta Crystallographica Section F
**Structural Biology and Crystallization Communications**
ISSN 1744-3091

# The purification, crystallization and preliminary structural characterization of human MAWDBP, a member of the phenazine biosynthesis-like protein family

**Petra Herde and Wulf Blankenfeldt***

Max-Planck-Institute of Molecular Physiology, Otto-Hahn-Strasse 11, 44227 Dortmund, Germany

Correspondence e-mail: wulf.blankenfeldt@mpi-dortmund.mpg.de

Received 27 February 2006
Accepted 28 April 2006

MAWDBP is the only representative of the phenazine biosynthesis-like protein family in the human genome. Its expression is elevated in several disease processes, including insulin resistance, folate deficiency and hypotension, and it may also be involved in carcinogenesis. The exact molecular function of MAWDBP is unknown. Native and seleno-L-methionine-labelled MAWDBP were expressed in *Escherichia coli* and crystallized at room temperature from precipitants containing 10 m*M* KF, 14%(*w*/*v*) PEG 3350 and 0.1 *M* sodium citrate pH 5.4. Crystals belong to space group *H*32, with unit-cell parameters $a = b = 187$, $c = 241$ Å, indicative of three to five monomers per asymmetric unit. Crystals were cryoprotected with 15%(*v*/*v*) glycerol and data have been collected to 2.7 Å resolution.

## 1. Introduction

The phenazine biosynthesis-like proteins define a newly emerging enzyme family for which structural and functional knowledge is still scarce. Only one representative of this family, 'MAWD-binding protein' (MAWDBP), is encoded in the human genome. MAWDBP, sometimes termed MAWBP in the literature, was first identified as a binding partner of the 'putative human mitogen-activated protein kinase (MAPK) activator with WD repeats' (hMAWD) in a two-hybrid screen using residues 214–350 of hMAWD as a bait (Iriyama *et al.*, 2001). hMAWD is a WD-40 repeat-containing $\beta$-propeller protein believed to participate in an MAPK signalling pathway. As elevated expression of hMAWD has been observed in breast cancer cells (Matsuda *et al.*, 2000), the activity of MAWDBP may be linked to tumour progression. MAWDBP is expressed in most tissues, indicating that the protein is involved in basic cellular functions (Iriyama *et al.*, 2001). Recent reports have described increased levels of MAWDBP mRNA or protein in the liver of rats after dietary folate deficiency (Chanson *et al.*, 2005), in hepatitis B and C viral infection (Kurokawa *et al.*, 2004), in insulin resistance (Solomon *et al.*, 2005) and in the kidney after hypotension (Westhoff *et al.*, 2005).

The exact molecular function of MAWDBP is unknown. Related proteins such as phenazine-biosynthesis protein PhzF (overall sequence identity according to the structure-based sequence alignment shown in Fig. 1 is 21%; Blankenfeldt *et al.*, 2004; Parsons *et al.*, 2004), diaminopimelate epimerase DapF (sequence identity 11%; Cirilli *et al.*, 1998) or the pyridoxal phosphate-independent *Trypanosoma cruzi* proline racemase TcPRACA (sequence identity 9%; Buschiazzo *et al.*, 2006) convert amino-acid-like substrates *via* acid/base catalytic mechanisms. A hallmark of these enzymes is their structural symmetry, which arises from gene duplication and yields two similar domains that give the monomer a butterfly shape. DapF and TcPRACA require two cysteines on opposite sites of their active centre for catalysis (Cys73 and Cys217, DapF numbering), which act as base and acid, respectively. Each of the two homologous domains contributes one of these cysteines from equivalent sequence positions. In contrast, cysteine residues are not found in the active site of PhzF and a glutamic acid (Glu45, PhzF numbering) instead carries out a prototropic shift reaction (Blankenfeldt *et al.*, 2004). Several mixed-type family members with only one of the two active-site

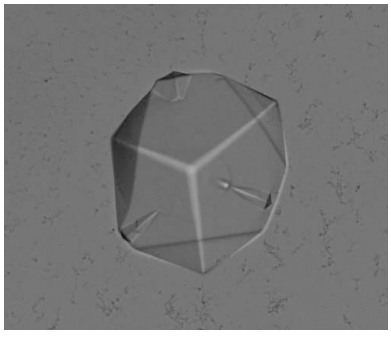

cysteines of DapF/TcPRACA but all of the conserved active-site residues of PhzF (Glu45, His74, Asp208) have been identified and representative structures have been determined by structural genomics initiatives, albeit without further experimental functional characterization. The *Escherichia coli* protein YddE (sequence identity 22%) contains a cysteine residue in its N-terminal domain (Blankenfeldt *et al.*, 2004; Grassick *et al.*, 2004), whereas the recently reported yeast protein YHI9 (sequence identity 20%) is the first structure of a subfamily containing only the active-site cysteine of the C-terminal domain (Liger *et al.*, 2005). MAWDBP belongs to the YddE group (Fig. 1). To gain further insight into this interesting enzyme family, we have initiated structural and functional characterization of this single member of the PhzF fold in the human genome.

## 2. MAWDBP overexpression and purification

cDNA of human MAWDBP was retrieved from RZPD (Deutsches Ressourcenzentrum für Genomforschung GmbH, Berlin, Germany; clone IRAT p970F059D6) and amplified by PCR with primers MAWDBP-forw-NdeI (5′-CTT GCA AGG CAT ATG AAG CTT CCT ATT TCC-3′) and MAWDBP-rev-BamHI (5′-AGC ATA GGA TCC TCT AGG CTG TCA GTG TG-3′). The PCR product was digested with *Nde*I and *Bam*HI, and ligated into pET15b (Novagen) previously treated in the same manner. The resulting construct encodes MAWDBP fused to an N-terminal $His_6$ tag that can be cleaved off with thrombin. It was sequenced and transformed into *E. coli* Rosetta (DE3) pLysS (Novagen). Cells were grown at 310 K in Terrfic Broth supplemented with 100 mg $l^{-1}$ ampicillin and 34 mg $l^{-1}$ chloramphenicol until $OD_{600}$ reached 0.6. At this stage, the temperature was reduced to 293 K and the culture was induced overnight with 0.5 m*M* isopropyl $\beta$-D-thiogalactopyranoside (IPTG). Cells were harvested by centrifugation and resuspended in lysis buffer [300 m*M* NaCl, 50 m*M* $Na_2HPO_4$ pH 8.0, 10%(*v*/*v*) glycerol] supplemented with 1 m*M* PMSF for cell disruption in a microfluidizer. The lysate was cleared by ultracentrifugation at 150 000*g* and the resulting supernatant applied onto a HiTrap Chelating HP column (GE Healthcare Life Sciences) charged with 100 m*M* $NiSO_4$. Weakly bound protein was eluted with a lysis buffer containing 2 m*M* imidazole. The imidazole concentration was then gradually increased and MAWDBP eluted at a concentration of ∼200 m*M*. Pure fractions were identified by SDS–PAGE, pooled and the buffer was exchanged to 20 m*M* Tris–HCl pH 8.0, 150 m*M* NaCl, 10%(*v*/*v*) glycerol with a HiPrep-Desalting column (GE Healthcare Life Sciences). At this stage removal of the N-terminal $His_6$ tag with thrombin was attempted, but only partial cleavage could be achieved. Thrombin cleavage was therefore not pursued further in consecutive batches. The purified protein was subjected to size-exclusion chromatography on Superdex S75 (GE Healthcare Life Sciences) in 20 m*M* Tris–HCl pH 8.0, 150 m*M* NaCl, 10%(*v*/*v*) glycerol. MAWDBP eluted with an apparent molecular weight of 48 kDa, which is in between the expected weight of a monomer and a dimer. A similar behaviour was observed for PhzF, which was subsequently found to be dimeric (Blankenfeldt *et al.*, 2004), indicating that native MAWDBP is likely to also be a dimer. The typical yield was 100 mg per litre of culture as determined by Bradford assay (Bradford, 1976). Pure protein was concentrated to 10 mg $ml^{-1}$ and small aliquots were flash-frozen in liquid nitrogen for long-term storage.

Seleno-L-methionine labelling was achieved by inhibition of methionine biosynthesis (Doublié, 1997). Bacteria were grown in LeMaster media (Hendrickson *et al.*, 1990) supplemented with 33 mg $l^{-1}$ ampicillin and 11 mg $l^{-1}$ chloramphenicol until $OD_{600}$ reached 0.5. At this stage seleno-L-methionine (60 mg $l^{-1}$) was added and protein expression was induced for 3 h at 310 K by addition of 1 m*M* IPTG. Incorporation of the label was confirmed by MALDI mass spectroscopy. The labelled protein had identical purification properties to the wild type.

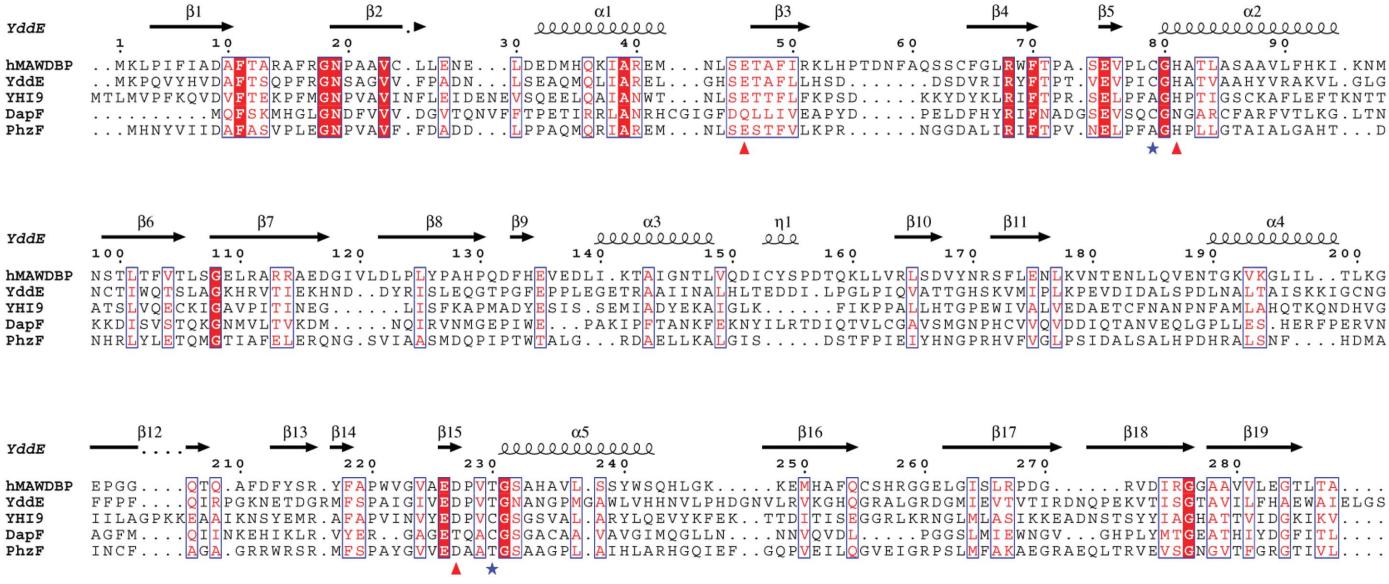


**Figure 1**
Sequence alignment of human MAWDBP and representative related proteins whose structures have been deposited in the Protein Data Bank (PDB; Berman *et al.*, 2000), namely YddE from *E. coli*, YHI9 from yeast, DapF from *Haemophilus influenza* and PhzF from *Pseudomonas fluorescens* 2-79. The alignment is based on a structural superimposition of DapF (PDB code 1bwz) and PhzF (PDB code 1xub). Secondary-structure elements of YddE (PDB code 1sdj), which is likely to be the closest functional relative of MAWDBP, have been calculated with *DSSP* (Kabsch & Sander, 1983) and are given at the top of each block. Conserved residues are highlighted with a red background and positions with structurally conservative substitution higher than 70% (Risler *et al.*, 1988) are printed in red and surrounded by a blue box. Active-site cysteines in DapF (positions 79 and 230) are indicated with a blue asterisk and the conserved active-site residues of PhzF (positions 46, 81 and 227) are indicated with a red triangle. The figure was prepared with *ESPript* (Gouet *et al.*, 2003).

## 3. MAWDBP crystallization

Initial crystallization conditions were determined at room temperature using Crystal Screen, Crystal Screen II and the PEG/Ion Screen from Hampton Research in 100 nl protein solution plus 100 nl reservoir solution sitting drops set up against 100 µl reservoir solution with a Mosquito nanolitre dispensing robot (Molecular Dimensions Ltd). The protein concentration was tested at 5, 10 and 20 mg ml$^{-1}$. Crystals appeared after 3 h with precipitants from the PEG/Ion Screen containing PEG 3350 and fluoride salts. The screens were therefore repeated with protein preincubated with 10 m*M* KF, but no principally new crystal forms were detected. The initial conditions were therefore optimized with respect to protein concentration, precipitant composition and pH. In addition, the setup was changed to hanging drop in order to produce larger crystals for data collection. Pyramidal crystals (∼150 × 150 × 50 µm) appeared after 3 d at room temperature with 10 mg ml$^{-1}$ MAWDBP, 14%(*w*/*v*) PEG 3350, 0.1 *M* sodium citrate pH 5.4 and 10 m*M* KF (Fig. 2). The drop size was increased to 2.5 µl protein solution plus 2.5 µl precipitant to counteract drop spreading on the cover slips owing to glass etching by fluoride at this acidic pH. The reservoir volume was 500 µl. The low amount of fluoride essential for crystallization is likely to indicate specific binding to MAWDBP, similar to PhzF, which required low concentrations of anions such as sulfate, phosphate, acetate or tartrate for crystallization of the apo form (Mavrodi *et al.*, 2004). These anions were later found to bind to the active centre of the enzyme and neutralize the repulsion of the positive poles of the central α-helices pointing towards each other from the two domains contained in the monomer (Blankenfeldt *et al.*, 2004; Parsons *et al.*, 2004).

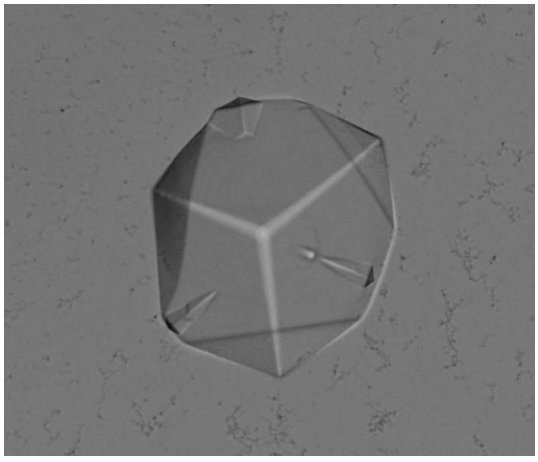

**Figure 2**
Crystal of human MAWDBP showing typical satellite growth.

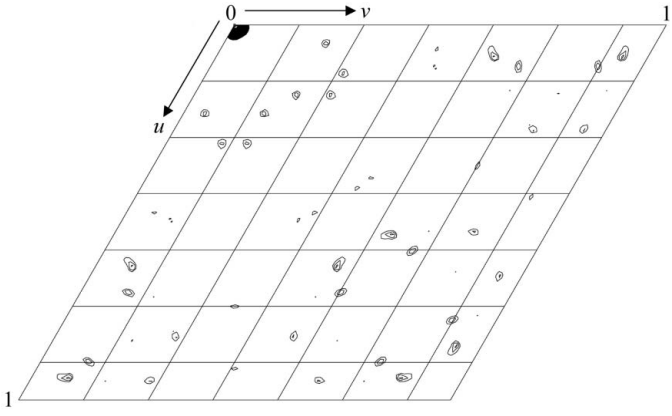


**Figure 3**
Harker section $w$ = 0 of the Patterson map calculated with the anomalous differences of the SAD data (all data included, map contoured at 2.2$\sigma$). The figure was prepared with the graphical interface to the *CCP*4 program suite (Potterton *et al.*, 2003).

**Table 1**
Data-collection statistics.

Data were collected at X10SA of the Swiss Light Source (Villigen, Switzerland). Values in parentheses are for the highest resolution shell.

| | Native | SeMet SAD |
|---|---|---|
| Wavelength (Å) | 0.95 | 0.95 |
| Resolution | 20–2.6 (2.7–2.6) | 20–3.0 (3.1–3.0) |
| Space group | *H*32 | *H*32 |
| Unit-cell parameters (Å) | $a = b = 187.3$, $c = 240.8$ | $a = b = 186.8$, $c = 239.5$ |
| Total measurements | 233982 | 839339 |
| Unique reflections | 49719 | 32181 |
| Average redundancy | 4.7 (4.7) | 26.1 (25.6) |
| $I/\sigma(I)$ | 14.4 (4.0) | 35.2 (9.5) |
| Completeness (%) | 99.5 (100) | 99.6 (100) |
| Anomalous completeness† (%) | — | 99.6 (100) |
| Wilson $B$ (Å$^2$) | 58 | 60 |
| $R_{\rm sym}$‡ | 6.8 (42.5) | 8.6 (48.7) |

† Completeness calculations treat Friedel pairs as separate observations. ‡ $R_{\rm sym} = \sum |I(h)_j - \langle I(h)\rangle| / \sum I(h)_j$, where $I(h)_j$ is the scaled observed intensity of the $i$th symmetry-related observation of reflection $h$ and $\langle I(h)\rangle$ is the mean value.

## 4. Data collection

Prior to data collection, MAWDBP crystals were briefly washed in mother liquor supplemented with 15%(*v*/*v*) glycerol and flash-cooled in liquid nitrogen. Data were collected at 100 K. The crystals belong to space group *H*32, with unit-cell parameters $a = b = 187$, $c = 241$ Å, $\alpha = \beta = 90$, $\gamma = 120^\circ$, indicating the presence of three to five MAWDBP monomers in the asymmetric unit (solvent content 68–46%). They are relatively soft and have a strong tendency to form satellite crystals (Fig. 2), which is not always immediately obvious from their shape but becomes apparent from independent diffraction patterns present in the oscillation images. It was necessary to screen ∼20 crystals to find one that was singular. Native and selenomethionine-labelled crystals behaved similarly; however, the labelled crystals diffracted more weakly. Data-collection statistics are given in Table 1.

Native data at cryogenic temperature were collected to 2.6 Å resolution on beamline X10SA of the Swiss Light Source (SLS, Villigen, Switzerland). Data were indexed, integrated and merged with *XDS* (Kabsch, 1993). As molecular replacement with related structures was not successful, experimental phasing with anomalous data has been initiated. To balance between maximal anomalous differences and minimal radiation damage (Leonard *et al.*, 2005), a highly redundant data set consisting of 600 0.7° rotation images was collected to 3.0 Å resolution at 12.59 keV, above the *K* absorption edge of selenium. The X-ray beam was highly attenuated to minimize radiation damage. The Harker sections of the anomalous differences Patterson map reveal the presence of several anomalous scatterers (Fig. 3). We are currently using these data for phase determination. The structure of MAWDBP together with functional data will be published elsewhere.

We would like to thank Eckhard Hofmann, Olena Pylypenko, Ilme Schlichting and Andrea Scrima for help with data collection, Melanie

Baumann for excellent technical assistance and Roger S. Goody for his support. Access to beamline X10SA (PXII) at the Swiss Light Source, Villigen, Switzerland is gratefully acknowledged.

## References


Berman, H. M., Westbrook, J., Feng, Z., Gilliland, G., Bhat, T. N., Weissig, H., Shindyalov, I. N. & Bourne, P. E. (2000). *Nucleic Acids Res.* **28**, 235–242.

Blankenfeldt, W., Kuzin, A. P., Skarina, T., Korniyenko, Y., Tong, L., Bayer, P., Janning, P., Thomashow, L. S. & Mavrodi, D. V. (2004). *Proc. Natl Acad. Sci. USA*, **101**, 16431–16436.

Bradford, M. M. (1976). *Anal. Biochem.* **72**, 248–254.

Buschiazzo, A., Goytia, M., Schaeffer, F., Degrave, W., Shepard, W., Gregoire, C., Chamond, N., Cosson, A., Berneman, A., Coatnoan, N., Alzari, P. M. & Minoprio, P. (2006). *Proc. Natl Acad. Sci. USA*, **103**, 1705–1710.

Chanson, A., Sayd, T., Rock, E., Chambon, C., Sante-Lhoutellier, V., Potier de Courcy, C. & Brachet, P. (2005). *J. Nutr.* **135**, 2524–2529.

Cirilli, M., Zheng, R., Scapin, G. & Blanchard, J. S. (1998). *Biochemistry*, **37**, 16452–16458.

Doublié, S. (1997). *Methods Enzymol.* **276**, 523–530.

Gouet, P., Robert, X. & Courcelle, E. (2003). *Nucleic Acids Res.* **31**, 3320–3323.

Grassick, A., Sulzenbacher, G., Roig-Zamboni, V., Campanacci, V., Cambillau, C. & Bourne, Y. (2004). *Proteins*, **55**, 764–767.

Hendrickson, W. A., Horton, J. R. & LeMaster, D. M. (1990). *EMBO J.* **9**, 1665–1672.

Iriyama, C., Matsuda, S., Katsumata, R. & Hamaguchi, M. (2001). *J. Hum. Genet.* **46**, 289–292.

Kabsch, W. (1993). *J. Appl. Cryst.* **26**, 795–800.

Kabsch, W. & Sander, C. (1983). *Biopolymers*, **22**, 2577–2637.

Kurokawa, Y., Matoba, R., Nakamori, S., Takemasa, I., Nagano, H., Dono, K., Umeshita, K., Sakon, M., Monden, M. & Kato, K. (2004). *J. Exp. Clin. Cancer Res.* **23**, 135–141.

Leonard, G. A., Sainz, G., de Backer, M. M. & McSweeney, S. (2005). *Acta Cryst.* D**61**, 388–396.

Liger, D., Quevillon-Cheruel, S., Sorel, I., Bremang, M., Blondeau, K., Aboulfath, I., Janin, J., van Tilbeurgh, H. & Leulliot, N. (2005). *Proteins*, **60**, 778–786.

Matsuda, S., Katsumata, R., Okuda, T., Yamamoto, T., Miyazaki, K., Senga, T., Machida, K., Thant, A. A., Nakatsugawa, S. & Hamaguchi, M. (2000). *Cancer Res.* **60**, 13–17.

Mavrodi, D. V., Bleimling, N., Thomashow, L. S. & Blankenfeldt, W. (2004). *Acta Cryst.* D**60**, 184–186.

Parsons, J. F., Song, F., Parsons, L., Calabrese, K., Eisenstein, E. & Ladner, J. E. (2004). *Biochemistry*, **43**, 12427–12435.

Potterton, E., Briggs, P., Turkenburg, M. & Dodson, E. (2003). *Acta Cryst.* D**59**, 1131–1137.

Risler, J. L., Delorme, M. O., Delacroix, H. & Henaut, A. (1988). *J. Mol. Biol.* **204**, 1019–1029.

Solomon, S. S., Buss, N., Shull, J., Monnier, S., Majumdar, G., Wu, J. & Gerling, I. C. (2005). *J. Lab. Clin. Med.* **145**, 275–283.

Westhoff, T. H., Scheid, S., Tolle, M., Kaynak, B., Schmidt, S., Zidek, W., Sperling, S. & van der Giet, M. (2005). *Physiol. Genomics*, **23**, 46–53.